Revised Version

Supporting Information

Viedma deracemization mechanisms in self-assembly processes

Josep. M. Ribó[a], David Hochberg † [b], Thomas Buhse[c], Jean-Claude Micheau[d]

(a): Department of Organic and Inorganic Chemistry, Institute of Cosmos Science (IEEC-UB), University of Barcelona, E-08028 Barcelona, Catalonia, Spain. orcid.org/0000-0001-6258-1726; E-mail: jmribo@ub.edu;

(b): Department of Molecular Evolution, Centro de Astrobiología (CSIC-INTA), Carretera Ajalvir Kilómetro 4, E-28850 Torrejón de Ardoz, Madrid, Spain. orcid.org/0000-0002-0411-019X; E-mail: hochbergd@cab.inta-csic.es

(c): Centro de Investigaciones Químicas, IICBA, Universidad Autónoma del Estado de Morelos, 62209 Cuernavaca, Morelos, Mexico.
orcid.org/0000-0001-5082-0873; E-mail: buhse@uaem.mx

(d): Laboratoire Softmat, UMR au CNRS n° 5623, Université Paul Sabatier, F-31062 Toulouse, France.
orcid.org/0000-0002-1193-4306; E-mail: jean-claude.micheau@univ-tlse3.fr

1. Comparison of the complete and compact models and the MG, and CG mechanisms

line	process	complete	compact	*monomer growth part* (MG)	*cluster growth part* (CG)
1	A + A ⇄ C2	yes	yes	*yes*	*yes*
2	A + C2 ⇄ C3	yes	no	*yes*	*no*
3	A + C3 ⇄ C4	yes	no	*yes*	*no*
4	A + C4 ⇄ C5	yes	no	*yes*	*no*
5	A + C5 ⇄ C6	yes	no	*yes*	*no*
6	A + C6 ⇄ C7	yes	yes	*yes*	*no*
7	A + C7 ⇄ C8	yes	yes	*yes*	*no*
8	C2 + C2 ⇄ C4	yes	yes	*no*	*yes*
9	C2 + C4 ⇄ C6	yes	yes	*no*	*yes*
10	C2 + C6 ⇄ C8	yes	yes	*no*	*yes*
11	C4 + C4 ⇄ C8	yes	no	*no*	*no*
12	C8 -> C4 + C4	no/yes	no/yes	no/yes	no/yes

Table 1S: List of processes included in our models and mechanisms. Dimerization is on line 1 as C = L or D, this step is also a racemization. Line 1 is common step for all models, complete, compact, MG and CG. From line 2 to line 7 are gathered the so-called monomer growth processes: the reversible addition/elimination of one achiral monomer (MG mechanism). From line 8 to 10 are the so-called cluster growth: the reversible addition/elimination of a smaller aggregate on a larger aggregate, here the smaller aggregate is a dimer (CG mechanism). The complete model comprises all these steps while some of them are neglected in the compact model (see lines 2 to 5). The irreversible grinding is shown in magenta on line 12.

2. SNA analysis of the complete model scenario and MG and CG mechanisms

MG	MG + Grinding	CG	CG + Grinding	MG + CG Same EFMs than those of MG and CG alone plus following EFMs	MG + CG + Grinding Same EFMs than MG + CG plus following EFMs
A + A -> C2 C2 -> A +A	A + A -> C2 C2 -> A +A	A + A -> C2 C2 -> A + A	A + A -> C2 C2 -> A + A	A + A -> C2 C2 +C6 -> C8 C8 -> A + C7 C7 -> A + C6	C2 + C4 -> C6 C2 + C6 -> C8 C8 -> C4 + C4 C4 -> C2
A + C2 -> C3 C3 -> A + C2	A + C2 -> C3 C3 -> A + C2	C2 + C2 -> C4 C4 -> C2 + C2	C2 + C2 -> C4 C4 -> C2 + C2	A + A -> C2 C2 +C4 -> C6 C6 -> A + C5 C5 -> A + C4	C2 + C4 -> C6 A + C6 -> C7 A + C7 -> C8 C8 -> C4 + C4 C4 -> A + C3 C3 -> A + C2
A + C3 -> C4 C4 -> A + C3	A + C3 -> C4 C4 -> A + C3	C2 + C4 -> C6 C6 -> C2 + C4	C2 + C4 -> C6 C6 -> C2 + C4	A + A -> C2 C2 + C2 -> C4 C4 -> A +C3 C3 -> A + C2	A + C4 -> C5 A + C5 -> C6 C2 + C6 -> C8 C8 -> C4 + C4 C4 -> A + C3 C3 -> A + C2
A + C4 -> C5 C5 -> A + C4	A + C4 -> C5 C5 -> A + C4	C2 + C6 -> C8 C8 -> C2 + C8	C2 + C6 -> C8 C8 -> C2 + C8	A + C6 -> C7 A + C7 -> C8 C8 -> C2 + C6 C2 -> A + A	A + A -> C2 C2 + C4 -> C6 C2 + C6 -> C8 C8 -> C4 + C4 C4 -> A + C3 C3 -> A + C2
A + C5 -> C6 C6 -> A + C7	A + C5 -> C6 C6 -> A + C7		C2 + C4 -> C6 A2 + C8 -> C8 C8 -> C4 + C4 C4 -> C2 + C2	A + C4 -> C5 A + C5 -> C6 C6 -> C2 + C4 C2 -> A + A	C2 + C4-> C6 A + C6 -> C7 A + C7 -> C8 C8 -> C4 + C4 C4 -> C2 + C2 C2-> A + A
A + C6 -> C7 C7 -> A + C6	A + C6 -> C7 C7 -> A + C6			A + C2 -> C3 A + C3-> C4 C4 –> C2 + C2 C2-> A+ A	A + C4 -> C5 A + C5 -> C6 C2 + C6 -> C8 C8 -> C4 + C4 C4 -> C2 + C2 C2 -> A + A
A + C7 -> C8 C8 -> A + C7	A + C7 -> C8 C8 -> A + C7			A + C4 -> C5 A + C5 -> C6 C2 + C6 -> C8 C8 -> A + C7 C7 -> A + C6 C6 -> C2 + C4	A + C4 -> C5 A + C5 -> C6 A + C6 -> C7 A + C7 -> C8 C8 -> C4 + C4 C4 -> C2 + C2 C2 -> A + A
	A + C4 -> C5 A + C5 -> C6 A + C6 -> C7 A + C7 -> C8 C8 -> C4 + C4 C4 -> A + C3 C3 -> A + C2 C2 -> A + A			A + C2 –> C3 A + C3 -> C4 C2 + C6 -> C8 C8 -> A + C7 C7 -> A + C6 C4 -> C2 + C2	A + C4 -> C5 A + C5 -> C6 A + C6 -> C7 A + C7 -> C8 C8 -> C4 + C4 C4 -> A + C3 C3 -> A + C2 C2 -> A + A
				A + C6 -> C7 A + C7 -> C8 C2 + C4 -> C6 C8 -> C2 + C6 C6 -> A + C5 C5 -> A + C4	A + C4 -> C5 A + C5 -> C6 C2 + C6 -> C8 C8 -> C4 + C4 C8 -> A + C7 C7 -> A + C6 C4 -> C2 + C2
				A + C6 -> C7 A + C7 -> C8 C2 + C2 -> C4 C8 -> C2 + C6 C4 -> A + C3 C3 -> A + C2	C2 + C4 -> C6 A + C6 -> C7 A + C7 -> C8 C8 -> C4 + C4 C6 -> A + C5 C5 -> A + C4 C4 -> C2 + C2
				C2 + C2 -> C4 A + C4 -> C5 A + C5 -> C6 C6 -> C2 + C4 C4 -> A + C3 C3 -> A + C2	C2 + C2 -> C4 A + C4 -> C5 A + C5 -> C6 A + C6 -> C7 A + C7 -> C8 C8 -> C4 + C4 C4 -> A + C3 C3 -> A + C2
				A + C2 -> C3 A + C3 -> C4 C2 + C4 -> C6 C6 -> A + C5 C5 -> A + C4 C4 -> C2 + C2	
Thermodynamic Equilibrium	No SMSB Stable Racemic NESS	Thermodynamic Equilibrium	No SMSB Stable Racemic NESS	Thermodynamic Equilibrium	SMSB can occur

Table 2SI. EFMs for the three kinetic scenarios of monomer-to-cluster growth (MG mechanism), dimer-to-cluster growth (CG mechanism), the mixed system of MG + CG mechanisms, and under the effect of irreversible grinding (C8 -> C4 + C4). Note the ability or not for the systems to show SMSB when grinding is acting. This occurs only in the MG + CG scenario (the so-called complete model). The coupling of both growth mechanisms in the MG + CG scenario leads to the formation of polymerization-depolymerization cycles, leading to an autocatalytic dynamic in the formation of chiral matter. The inclusion of the grinding reaction determines in these cycles a net flow in the sense of grinding and rebuilding of C8 and the presence of lateral depolymerizations arm (see Fig. 4 in main text) feeding the achiral A pool available for both chiral manifolds. The competition between these flows, for specific reaction parameters, can lead to the SMSB bifurcation.

3. Numerical simulation of a SMSB

Numerical integrations were carried out using the *Mathematica* software package to simulate SMSB from an unstable stationary state. The results were monitored and verified to ensure that the total system mass remained constant over time.

Numerical noise was minimized by setting a high numerical precision for the input parameters and using exact number representation for the reaction rates and initial concentration values. The fluctuations in chirality, which can convert the racemic output to an asymmetric one, were simulated by using an initial *ee* of products/catalysts lower than that predicted by statistical fluctuations of the ideal racemic composition. Specifically, an initial *ee*(%) < 67.43 x $(N_{part})^{-0.5}$, where N is the number of chiral molecules.[1,2]

Using this approach, SMSB was detected at initial *ee* values much lower than those expected from statistical fluctuations of the ideal racemic composition and in the absence of any parameter chiral polarization. In conditions where the initial chiral composition is ideally racemic or absent, no bias from the metastable racemic composition can be detected. The metastability was tested by applying the small chiral fluctuation value mentioned above making the system to deviate towards a stable SMSB.

Analogous results using this two-step simulation procedure were also obtained with *COPASI* (Version 4.44 – Build 295). In this case, the metastable racemic state was perturbed by applying an ee_o = 1e-7 to one of the chiral species concentrations, causing the system's trajectory to diverge from the original unstable stationary state and leading to a SMSB event.

4. Evaluation of the entropy production

Assuming ideal diffusion, perfect mixing and isothermal conditions the entropy production entropy ($dS/dt = P$) is due to the chemical reactions. This is the product of 1/T by the product of the chemical current (absolute rate) by the chemical force (Affinity) that originates it. When a reversible reaction is presented as composed by two unidirectional irreversible reactions such as it is the case of SNA, it results for example:

$A + D6 \longrightarrow D7;\ k_{3a}$ $\quad$ $D7 \longrightarrow A + D6;\ k_{m3a}$,

$$P_{3a} = R\, k_{3a}\, [A]\, [D_6] ln\left\{\frac{[A][D_6]}{[A]_{equil}[D_6]_{equil}}\right\}, \text{ and } \quad P_{m3a} = R\, k_{m3a}\, [D_7]\, ln\left\{\frac{[D_7]}{[D_7]_{equil}}\right\}.$$

In the case of the representation of the two former reactions as a reversible transformation, the addition of two former irreversible reactions leads to the common way of representation:[3]

$$P = \left(Rate_{forward} - Rate_{backward}\right) * ln\left\{\frac{Rate_{forward}}{Rate_{backward}}\right\}, \textit{ i.e.}$$

$A + D_6 \rightleftarrows D_7;\ K_{equil} = \frac{k_{3a}}{k_{m3a}}$ $\quad$ $P = R\left(k_{3a}[A][D_6] - k_{m3a}[D_7]\right) * ln\left\{\frac{k_{3a}[A][D_6]}{k_{m3a}[D_7]}\right\}$.

This means that the addition of both "irreversible" reactions evaluated in respect to the relative chemical potentials of the species in a system in thermodynamic equilibrium, is the same than the expression considering a reversible reaction pair.[3] All this, because the relative chemical potentials are:

$$\mu_k^{rel} = \left(\mu_k^0 + RTln[X_k]\right) - \left(\mu_k^0 + RTln[X_k]_{equil}\right) = RTln\left(\frac{[X_k]}{[X_k]_{equil}}\right).$$

Consideration of the relative chemical potentials allows the evaluation of the entropy production contribution of unidirectional "irreversible" reactions. For example, in continuous flow reactors, this is the entropy production evaluation of the matter exchange with the surroundings by the irreversible pseudo reactions of the entry and exit flows.[4] In the case of closed systems as those reported here, when the corresponding chemical potentials are known, because the thermodynamic constrain of the Wegscheider rule is fulfilled,[5,6] it allows the evaluation of entropy production of reaction cycles containing an irreversible path, such as it is the case of the irreversible transformation originated by cluster grinding. The corresponding chemical potentials can be inferred from the detailed balance constraints imposed in the model to all rate constants. In the case of the models of Table 1 and Table 1S the entropy production of the irreversible grinding path C8 => 2 C4, is e.g. for one enantiomer:

$$P_{gD_8} = R\, k_g\, [D_8] ln\left\{\frac{k_b[D_8]}{k_f[D_4]^2}\right\} = R\, k_g\, [D_8] ln\left\{\frac{k_{m3}k_{m4}k_2[D_8]}{k_3k_4k_{m2}[D_4]^2}\right\},$$

when the virtual equilibrium constant k_b/k_f is evaluated from the detailed balance of the other species. This means that when the representation of the right chemical potential of the species of a cycle containing an irreversible step is chemically correct, it fulfils the Wegscheider condition.[5] The exchange entropy term P_{gD_8} must at the stationary state exactly balance the internal entropy production of the rest of transformations, in agree with the thermodynamic constraint $P_{int} = -P_{exch}$.[7] Table 3SI and Fig. 1SI below correspond to the same parameter set that the case of Fig. 6 of the main text.

Table 3SI. Total entropy production values of the instable racemic NESS and of the stable scalemic NESS in the compact model, showing the balance between internal entropy production and that originated by the the grinding of C8 clusters. In magenta the contributions of the grinding breaking reaction to the exchange entropy flow. Kinetic and other system parameters as those of the main text.

Reaction	Unstable Racemic NESS	Stable Scalemic NESS (*ee* = 98.2 %)
1) $2A \Leftrightarrow D_2$	0.076	0.097
2) $2A \Leftrightarrow L_2$	0.076	3.4×10^{-8}
3) $D_2 \Leftrightarrow D_4$	3.015	7.034
4) $L_2 \Leftrightarrow L_4$	3.015	9.3×10^{-6}
5) $D_2 + D_4 \Leftrightarrow D_6$	0.164	0.330
6) $L_2 + L_4 \Leftrightarrow L_6$	0.164	7.7×10^{-6}
7) $D_2 + D_6 \Leftrightarrow D_8$	0.725	1.634
8) $L_2 + L_6 \Leftrightarrow L_8$	0.725	2.2×10^{-5}
9) $A + D_6 \Leftrightarrow D_7$	0.011	0.007
10) $A + L_6 \Leftrightarrow L_7$	0.011	1.4×10^{-5}
11) $A + D_7 \Leftrightarrow D_8$	0.008	0.005
12) $A + L_7 \Leftrightarrow L_8$	0.008	1.4×10^{-5}
$P_{int} = \sum_i P_{reaction\ i}$	7.99865	9.105555
D8 -> D4 + D4 $(P_{grindingD8})$	–3.99932	–9.10555
L8 -> L4 +L4 $(P_{grindingL8})$	–3.99932	$< -1 \times 10^{-5}$
$P_{exch} = P_{grindingD8} + P_{grindingL8}$	–7.99865	–9.10555

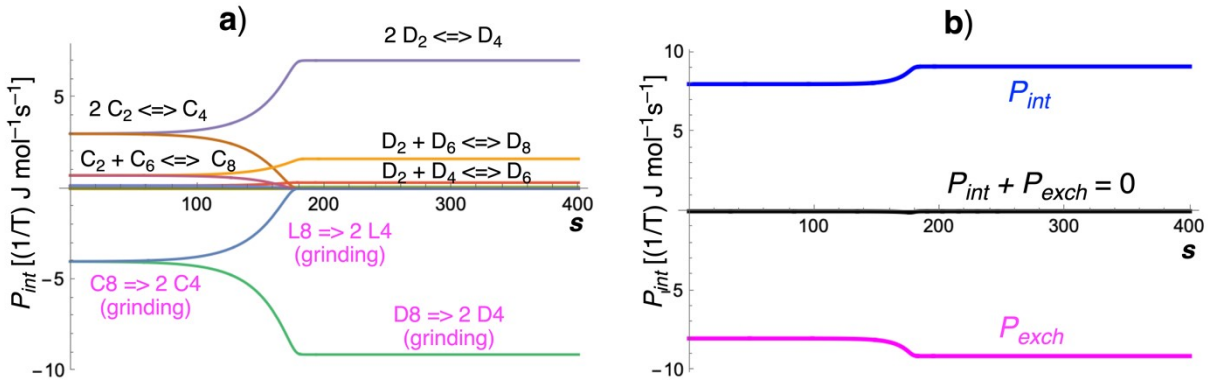

Figure 1SI. Time evolution of the entropy production in the transition from unstable racemic NESS to stable scalemic NESS of the compact model (case of Fig 6; initial and final values are shown in Table 3SI). a) Entropy production of the internal reversible reactions. b) Contribution of the grinding reaction to the exchange entropy flow. Total values differentiated the reversible internal transformation from the irreversible path of cluster grinding originated by the insulation of specific energy to yield C8 => 2 C4.

5. Dynamics *vs* kinetics of the internal autocatalytic network

According to Plasson et al.[8], autocatalysis achieves a quite different selectivity than that of the thermodynamic branch. For instance, there will be a bias from the racemic composition, in the case of enantioselective autocatalysis, if the system kinetics shows an adequate dynamic signature. Once the non-linear kinetics of the internal network dominates upon the linear kinetic parts, the autocatalysis dependence $\frac{d[X_i]}{dt} \propto [X_i]^n$ is manifested by the evolution dynamics. According to this previous report,[8] the figures below shows how the system acts in an autocatalytic way, either in the bias from the racemic composition (*ee*) or in the production of chiral matter. A significant point is the simple firs-order enantioselective autocatalysis achieved on the ee evolution. This effect is due to the instability of the racemic state. For chiral matter evolution, much higher autocatalytic orders are witnessed.

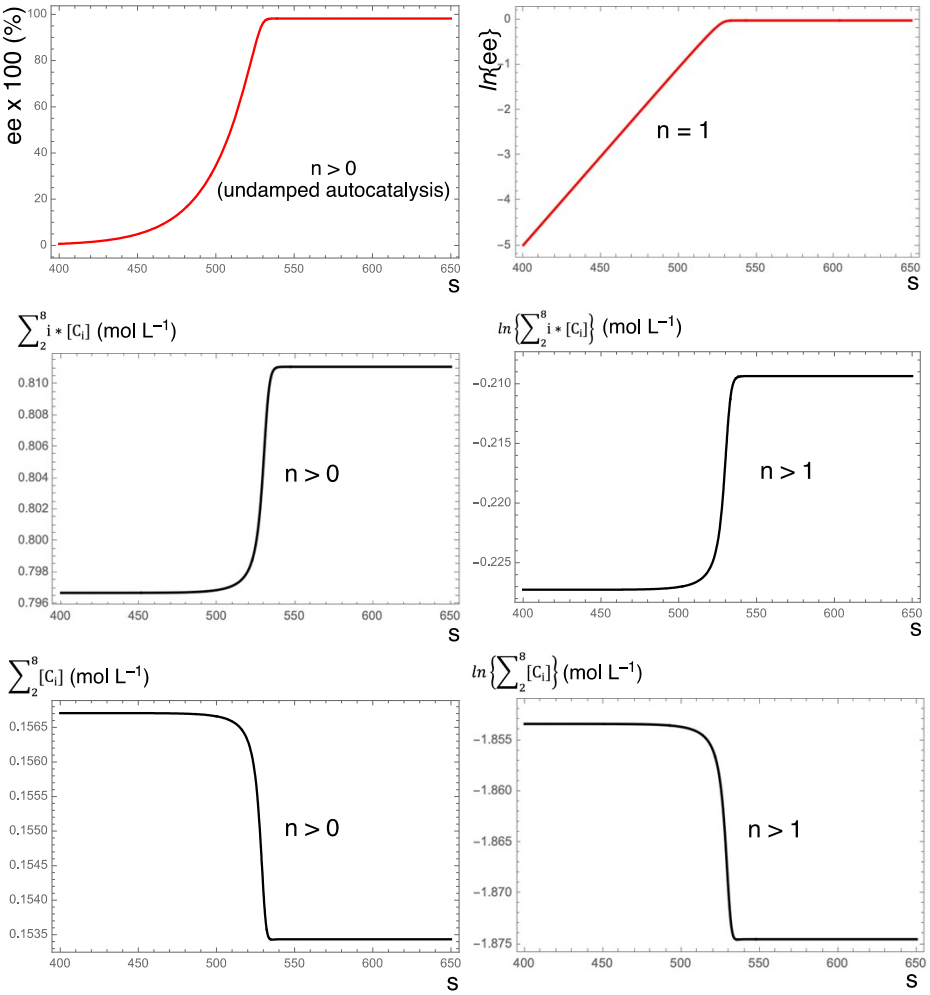

Figure 2SI. *First column:* evolution dynamics from the unstable racemic NESS to the stable scalemic NESS around the SMSB bifurcation point; from top to bottom, *ee*, chiral matter in mass, chiral matter in number. *Second column*: the technique to estimate the autocatalytic kinetic order is to use a log-scale to plot the same evolutions. while, the autocatalysis leading to the scalemic NESS remains of first order (linear evolution in log), the production of chiral matter gives rise to an autocatalytic order higher than 1 (sigmoidal evolution). This result is in agreement with the SNA showing the coupling and cycle formation between MG and CG reactions.

Supporting Information References

1 W. H. Mills, Some aspects of stereochemistry, *J. Soc. Chem. Ind.*, 1932, **51**, 750–759.

2 K. Mislow, Absolute Asymmetric Synthesis: A Commentary, *Collect. Czechoslov. Chem. Commun.*, 2003, **68**, 849–864.

3 D. Kondepudi and I. Prigogine, *Modern Thermodynamics*, Wiley, 2014.

4 D. Hochberg and J. M. Ribó, Stoichiometric network analysis of entropy production in chemical reactions, *Phys. Chem. Chem. Phys.*, 2018, **20**, 23726–23739.

5 A. N. Gorban and G. S. Yablonsky, Extended detailed balance for systems with irreversible reactions, *Chem. Eng. Sci.*, 2011, **66**, 5388–5399.

6 D. M. Stanbury and D. Hoffman, Systematic application of the principle of detailed balancing to complex homogeneous chemical reaction mechanisms, *J. Phys. Chem. A*, 2019, **123**, 5436–5445.

7 P. Glansdorff and I. Prigogine, *Thermodynamic theory of structure, stbility and fluctuations*, Wiley-Interscience, London, 1971.

8 R. Plasson, A. Brandenburg, L. Jullien and H. Bersini, Autocatalyses, *J. Phys. Chem. A*, 2011, **115**, 8073–8085.